ISSN 1070-3632, Russian Journal of General Chemistry, 2022, Vol. 92, No. 6, pp. 1056–1061. © Pleiades Publishing, Ltd., 2022.
Russian Text © The Author(s), 2022, published in Zhurnal Obshchei Khimii, 2022, Vol. 92, No. 6, pp. 981–987.

# Mechanically Activated Solid-State Synthesis of Nanocrystalline $Yb_4Zr_3O_{12}$

**A. M. Kalinkin[a],*, O. A. Kuz'menkov[a], E. V. Kalinkina[a], and V. V. Semushin[a]**

[a] *Tananaev Institute of Chemistry and Technology of Rare Elements and Mineral Raw Materials, Federal Research Center "Kola Scientific Center of the Russian Academy of Sciences", Apatity, 184209 Russia*
**e-mail: a.kalinkin@ksc.ru*

Received March 17, 2022; revised April 7, 2022; accepted April 10, 2022

**Abstract**—Nanocrystalline ytterbium zirconate $Yb_4Zr_3O_{12}$ (δ-phase) was synthesized by the solid-state method with preliminary mechanical activation of a stoichiometric mixture of the corresponding oxides. The processes occurring in the course of the synthesis were studied by X-ray powder diffraction, IR spectroscopy, and thermal analysis. The average size of $Yb_4Zr_3O_{12}$ crystallites obtained by annealing a mechanically activated oxide mixture at 900, 1000, 1100, and 1200°C was calculated by the Scherrer formula and was 12, 17, 27, and 41 nm, respectively.

**Keywords:** ytterbium zirconate, solid-state synthesis, mechanical activation, nanocrystalline state

**DOI:** 10.1134/S1070363222060172

Zirconates formed in the systems $Ln_2O_3$–$ZrO_2$ (where Ln is a rare earth) have been extensively used in recent years due to a combination of their valuable properties necessary for the preparation of thermal barrier coatings [1], electrolytes in solid oxide fuel cells [2], materials for radioactive waste immobilization [3], gas sensors [4], photocatalysts [5], and luminescence matrices [6]. The system $Yb_2O_3$–$ZrO_2$ includes solid solutions based on monoclinic and cubic $ZrO_2$, cubic $Yb_2O_3$, and one stoichiometric compound, $Yb_4Zr_3O_{12}$ (δ-phase) with rhombohedral structure (space group *R*-3) [7, 8]. At 1630°C, the rhombohedral structure of $Yb_4Zr_3O_{12}$ is transformed into defective fluorite structure (solid solution based on cubic $ZrO_2$) [7]. Thermodynamic modeling has been performed, and thermodynamic characteristics of phases in the system $Yb_2O_3$–$ZrO_2$ have been determined [9–12].

Wet chemistry methods and solid state synthesis have been applied to obtain $Yb_4Zr_3O_{12}$ (Table 1). Because of the low reaction rate, solid state syntheses are carried out at high temperatures (>1500°C) for a long time (up to several days) [13–16]. Wet chemistry methods based on calcination of precipitated hydroxides [12, 17, 18] or of the residue obtained after thermal decomposition of zirconium and ytterbium nitrates [8] make it possible to reduce the temperature of the process; however, the synthesis at 1000–1100°C lasts 4 months and longer. Combustion of the precursor prepared from a nitrate solution in the presence of citric acid provided milder conditions of the subsequent thermal treatment of the residue, but the synthesis of δ-$Yb_4Zr_3O_{12}$ was incomplete, and pelleting and annealing at 1525°C were necessary to complete the process [19]. The synthesis from oxides using a microwave plasma generator was characterized by a high temperature (up to 1910°C) and short time (tens of minutes), but additional calcination in a furnace at 1550°C for 24 h was required to obtain the ordered δ-phase [15]. The above considered methods are disadvantageous since the high temperature and/or prolonged thermal treatment favor increase of the size of $Yb_4Zr_3O_{12}$ crystallites, hamper formation of the product in the nanocrystalline state, and make it impossible to obtain nanosized ceramics with enhanced performance characteristics in comparison to microcrystalline analogs [20, 21].

An efficient way to accelerate solid state reactions consists of preliminary mechanical activation of the initial reactants in energy-intensive mills. Mechanical activation not only makes the mixture of reactants more homogeneous and increases their contact area but also gives rise to various structural defects [22–24], which

**Table 1.** Methods of synthesis of δ-$Yb_4Zr_3O_{12}$

| Method | Temperature, °C | Time | References |
|---|---|---|---|
| Sintering of precipitated hydroxides | 1400°C | 3–4 days | [18] |
| | 1000°C | ≥ 4 months | [17] |
| | 1500°C | Several hours | [12] |
| Calcination of the residue from thermal decomposition of zirconium and ytterbium nitrates | 1100°C | 517 days | [8] |
| Combustion of precursor | 850°C | 30 min in $O_2$ | [19] |
| Solid state synthesis | 1600°C | Several days | [13] |
| | 1500°C | 96 h | [14] |
| | 1550°C | 3×10-h cycles | [15] |
| | 1200°C | 200 h | [16] |
| | 1900°C | 5 h | [16] |
| Synthesis by microwave-induced plasma | 1450–1910°C | 5×10-min cycles | [15] |
| Solid state synthesis with mechanical activation | 1500°C | 6 h | [25] |

significantly intensifies the solid state synthesis upon further heating.

In the synthesis of $Yb_4Zr_3O_{12}$, the initial oxide mixture was mechanically activated in a Retsch PM 100 planetary ball mill using ceramic balls made of zirconium dioxide doped with yttrium oxide and grinding vials lined with the same ceramics [25]. After mechanical activation for 30 h, $Yb_4Zr_3O_{12}$ with defective fluorite structure was obtained. The ordered δ-phase was formed as a result of thermal treatment of the mechanically activated oxide mixture at 1500°C for 6 h. The size of the obtained δ-$Yb_4Zr_3O_{12}$ crystallites was not given, but the high temperature and long duration of sintering suggests that nanocrystalline compound was not formed.

An AGO-2 mill is one of the most efficient domestic and foreign planetary mills used for mechanical activation [26]. In comparison to the traditional solid state method, the temperature of the synthesis $La_2Zr_2O_7$ [27] and $Gd_2Zr_2O_7$ [28] can be reduced by 300–500°C due to preliminary mechanical activation of an oxide mixture in AGO-2.

We studied how mechanical activation of a stoichiometric mixture of Zr and Yb oxide in an AGO-2 planetary mill affects the solid state synthesis of nanocrystalline δ-$Yb_4Zr_3O_{12}$. According to the X-ray powder diffraction (XRD) data, mechanical activation over a period of 10 min leads to significant reduction of the peaks of ytterbium and zirconium oxides and their broadening, and the most part of low-intense peaks typical of the initial mixture disappears (Fig. 1). These findings suggest considerable structural defects and/or reduction in the size of $ZrO_2$ and $Yb_2O_3$ crystallites as a result of intense mechanical treatment in a planetary mill.

As in the case of the compositions $La_2O_3/ZrO_2$ [27] and $Gd_2O_3/ZrO_2$ [28], mechanical activation of a $Yb_2O_3/ZrO_2$ mixture involves hydration and carbonization of lanthanide oxide via reaction of $Yb_2O_3$ with atmospheric moisture and carbon dioxide. This follows from the appearance in the IR spectrum of the mechanically activated mixture of an O–H stretching band at 3440 $cm^{-1}$ and a doublet band at 1507/1400 $cm^{-1}$ due to $CO_3^{2-}$ stretchings (see Supplementary Materials).

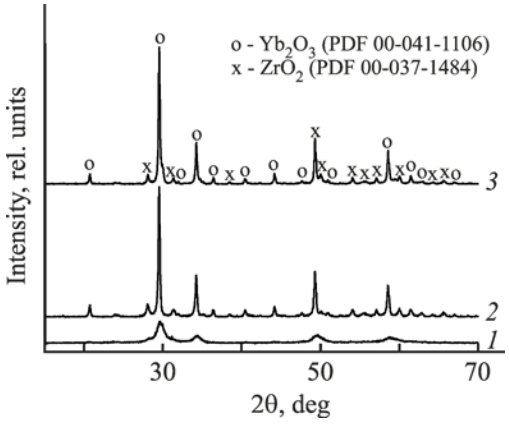


**Fig. 1.** X-Ray powder patterns of a mixture of zirconium and ytterbium oxides: (*1*) after mechanical activation, (*2*) initial mixture, (*3*) initial mixture after calcination at 1200°C for 3 h.

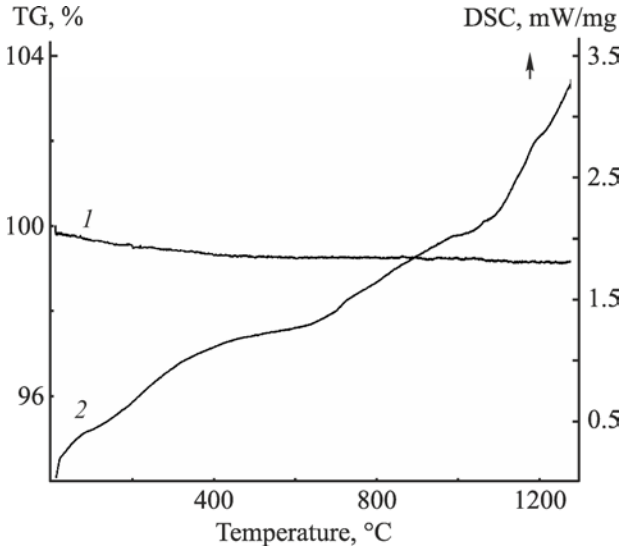


**Fig. 2.** (*1*) TG and (*2*) DSC curves of an initial mixture of zirconium and ytterbium oxides.

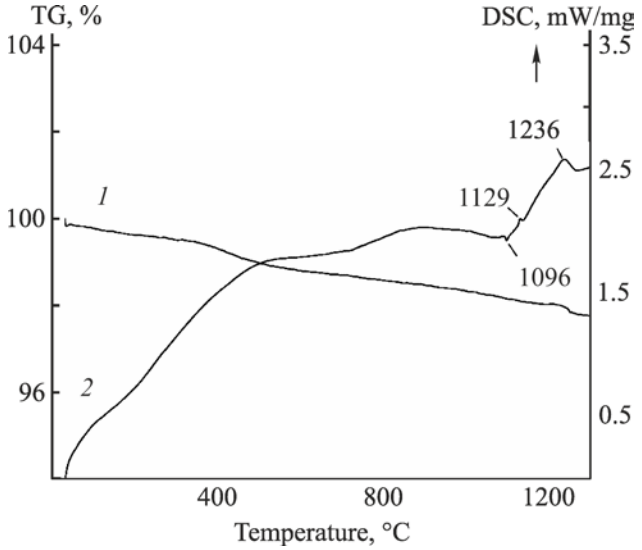


**Fig. 3.** (*1*) TG and (*2*) DSC curves of a mixture of zirconium and ytterbium oxides after mechanical activation.

Figures 2 and 3 show the differential scanning calorimetry (DSC) and thermogravimetric (TG) curves of the initial oxide mixtures before and after mechanical activation, respectively. The total weight loss of the initial mixture (0.89 wt %) is likely to result from dehydration and decarbonization. The DSC curve of the initial mixture lacks clearly defined endo- or exothermic effects (Fig. 2). This consistent with the XRD data (Fig. 1), according to which calcination of the initial $Yb_2O_3/ZrO_2$ mixture at 1200°C for 3 h was not accompanied by appearance of new phases.

The total weight loss of the mechanically activated mixture was appreciably larger (2.25 wt % according to the TG data; Fig. 3), which is related to dehydration and decarbonization processes, in keeping with the IR data (see Supplementary Materials). The DSC curve shape in the temperature range 1000–1300°C is likely to be determined by superposition of endothermic effects due to decomposition of carbonate groups and exothermic effects due to crystallization of amorphous Zr and Yb oxides, as well as of the exothermic effect due to start of formation of ytterbium zirconate. Presumably, the distinct exothermic DSC peak at 1236°C corresponds to crystallization of $Yb_4Zr_3O_{12}$, which (as follows from the TG data; Fig. 3) is accompanied by thermal decomposition of the residual carbonate groups. According to the IR data, complete decarbonization of the mechanically activated mixture is achieved after isothermal calcination at 1100°C for 3 h (see Supplementary Materials).

The X-ray powder patterns of the mechanically activated mixture after calcination at different temperatures are shown in Fig. 4. The δ-phase of $Yb_4Zr_3O_{12}$ crystallizes at a temperature of 1100°C and above. This follows from the appearance of additional reflections marked with arrows in Fig. 4. Elemental analysis showed that the mechanically activated mixture contains 0.9% of iron originating from abrasion of the mill balls and cylinder. The subsequent thermal treatment produces $YbFeO_3$ as an impurity phase (Fig. 4). To prevent contamination, it is advisable to carry out mechanical activation with the use of balls made of zirconium metal and zirconium-lined steel cylinders. In this case, the abraded material will be oxidized to one of the reactants ($ZrO_2$) during thermal treatment.

The effective size $D$ of $Yb_4Zr_3O_{12}$ crystallites was estimated from the broadening of the major diffraction peak at $2\theta = 29.89°$ using the Scherrer formula (1) [29].

$$D = \frac{\lambda}{B\cos\theta}. \quad (1)$$

Here, λ is the radiation wavelength, $B$ is the integral reflection width (in 2θ), and θ is the diffraction angle. The calculated size of ytterbium zirconate crystallites was 12,

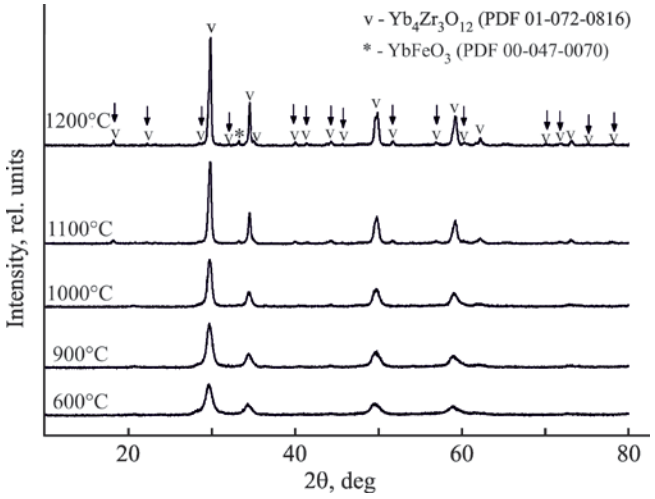


**Fig. 4.** X-Ray powder patterns of mechanically activated mixtures of zirconium and ytterbium oxides after calcination at different temperatures for 3 h.

17, 27, and 41 nm for samples obtained by sintering of the mechanically activated mixtures at 900, 1000, 1100, and 1200°C, respectively.

The SEM image of $Yb_4Zr_3O_{12}$ obtained by calcination of the mechanically activated mixture at 1100°C (see Supplementary Materials) shows polydisperse character of the powder and a tendency for particle aggregation. Large particles with a size of several micrometers are formed as a result of aggregation of primary particles most of which have a submicron size. The specific surface area of that sample was 1.48 $m^2/g$. The average size $D_S$ (nm) of $Yb_4Zr_3O_{12}$ particles was estimated from the calculated density (7.933 $g/cm^3$; PDF 01-072-0816) using formula (2). The $D_S$ value was 511 nm, which is consistent with the SEM data.

$$D_S = 6000/(\rho \cdot S_{sp}), \quad (2)$$

where ρ is the density ($g/cm^3$), and $S_{sp}$ is the specific surface area ($m^2/g$).

Thus, mechanical activation of a mixture of $Yb_2O_3$ and $ZrO_2$ in an AGO-2 centrifugal planetary mill for 10 min substantially accelerates the formation of $Yb_4Zr_3O_{12}$ upon subsequent sintering. Calcination of the mechanically activated mixture at 1100–1200°C for 3 h afforded nanocrystalline ytterbium zirconate. To the best of our knowledge, the nanocrystalline δ-phase of $Yb_4Zr_3O_{12}$ was not synthesized previously by the solid state method.

## EXPERIMENTAL

Zirconium oxide ($ZrO_2$) or pure grade was calcined at 600°C for 5 h, and ytterbium oxide ($Yb_2O_3$) of ultrapure grade (99.8%) was calcined at 900°C for 5 h. The specific surface areas of the initial oxides were determined by low-temperature nitrogen adsorption using a Flow-Sorb II 2300 analyzer (Micromeritics) and were 21.9 ($ZrO_2$) and 1.52 $m^2/g$ ($Yb_2O_3$).

A stoichiometric mixture of $ZrO_2$ and $Yb_2O_3$ was subjected to mechanical activation in an AGO-2 centrifugal planetary mill [30] in an air environment at a centrifugal factor of 40 g using steel vials and steel balls 8 mm in diameter. A grinding vial was charged with 10 g of an initial oxide mixture and 200 g of balls. The duration of mechanical activation was 10 min. To achieve macro-homogeneity of the resulting powders, the mill was turned off every 1 min, and the mixture was stirred with a metallic spatula. The initial and mechanically activated oxide mixtures were calcined in the temperature range from 600 to 1200°C for 3 h in a SNOL 6,7/1300 electrical furnace on exposure to air. The X-ray powder diffraction analysis was performed on a Shimadzu XRD 6000 diffractometer (Cu$K_\alpha$ radiation); the X-ray powder patterns were recorded with a step of 0.02° (2θ), and the signal accumulation time in each point was 1 s. Thermal analysis was carried out on a Netzsch STA 409 PC/PG. The oxide mixtures were heated in corundum crucibles to 1250°C under argon at a rate of 10 deg/min. Scanning electron microscopy was performed with a LEO-1450 microscope. The IR spectra were recorded on a Nicolet 6700 FT-IR Fourier spectrometer from samples prepared as KBr disks.

## AUTHOR INFORMATION

A.M. Kalinkin, ORCID: https://orcid.org/0000-0002-3668-8578

E.V. Kalinkina, ORCID: https://orcid.org/0000-0003-4538-0425

V.V. Semushin, ORCID: https://orcid.org/0000-0003-2456-3951

## CONFLICT OF INTEREST

A.M. Kalinkin is a member of the Editorial Board of the *Zhurnal Obshchei Khimii*. The other authors declare the absence of conflict of interest.

## SUPPLEMENTARY INFORMATION

The online version contains supplementary material vailable at https://doi.org/10.1134/S1070363222060172.

## REFERENCES


1. Zhao, Z.-T., Guo, R.-F., Mao, H.-R., and Shen, P., *J. Eur. Ceram. Soc*., 2021, vol. 41, p. 5768. https://doi.org/10.1016/j.jeurceramsoc.2021.04.053
2. Lyskov, N.V., Shchegolikhin, A.N., Stolbov, D.N., Kolbanev, I.V., Gomes, E., Abrantes, J.C.C., and Shlyakhtina, A.V., *Electrochim. Acta*, 2022, vol. 403, article no. 139632. https://doi.org/10.1016/j.electacta.2021.139632
3. Wang L., Li J., Xie H., Chen Q., Xie Y., Chen Q., Xie Y., *Prog. Nucl. Energy*, 2021, vol. 137, article ID 103774. https://doi.org/10.1016/j.pnucene.2021.103774
4. Zhong, F., Shi, L., Zhao, J., Cai, G., Zheng, Y., Xiao, Y., and Long, J., *Ceram. Int*., 2017, vol. 43, no. 15, p. 11799. https://doi.org/10.1016/j.ceramint.2017.06.019
5. Zinatloo-Ajabshir, S., Salavati-Niasari, M., Sobhari, A., and Zinatloo-Ajabshir, Z., *J. Alloys Compd*., 2018, vol. 767, p. 1164. https://doi.org/10.1016/j.jallcom.2018.07.198
6. Kumar, A., Singh, D.K., and Manam, J., *J. Mater. Sci.: Mater. Electron*., 2019, vol. 30, p. 2360. https://doi.org/10.1007/s10854-018-0509-8
7. Gonzalez, M., Moure, C., Jurado, J.R., and Duran, P., *J. Mater. Sci*., 1993, vol. 28, p. 3451. https://doi.org/10.1007/BF01159821
8. Kornienko, O.A., Andrievskaya, E.R., Bykov, A.I., and Bogatyreva, Zh.D., *Visn. Odes. Nats. Univ.: Khim*., 2018, vol. 23, no. 1 (65), p. 83. https://doi.org/10.18524/2304-0947.2018.1(65).124549
9. Fabrichnaya, O., Lakiza, S.M., Kriegel, M.J., Seidel, J., Savinykh, G., and Schreiber, G., *J. Eur. Ceram. Soc*., 2015, vol. 35, no. 10, p. 2855. https://doi.org/10.1016/j.jeurceramsoc.2015.03.037
10. Fabrichnaya, O. and Seifert, H.J., *CALPHAD: Comput. Coupling Phase Diagrams Thermochem*., 2010, vol. 34, no. 2, p. 206. https://doi.org/10.1016/j.calphad.2010.03.001
11. Stolyarova, V.L., Lopatin, S.I., Fabrichnaya, O.B., and Shugurov, S.M., *Rapid Commun. Mass Spectrom*., 2014, vol. 28, no. 1, p. 109. https://doi.org/10.1002/rcm.6764
12. Simoncic, P. and Navrotsky, A., *J. Am. Ceram. Soc*., 2007, vol. 90, no. 7, p. 2143. https://doi.org/10.1111/j.1551-2916.2007.01678.x
13. Thornber, M.R. and Bevan, D.J.M., *J. Solid State Chem*., 1970, vol. 1, nos. 1–4, p. 536. https://doi.org/10.1016/0022-4596(70)90139-8
14. Stecura, S., *Thin Solid Films*, 1987, vol. 150, no. 1, p. 15. https://doi.org/10.1016/0040-6090(87)90305-1
15. Chou, Y.H., Hondow, N., Thomas, C.I., Mitchell, R., Brydson, R., and Douthwaite, R.E., *Dalton Trans*., 2012, vol. 41, no. 8, p. 2472. https://doi.org/10.1039/C2DT12269C
16. Karaulov, A.G. and Zoz, E.I., *Refract. Ind. Ceram*., 1999, vol. 40, p. 479. https://doi.org/10.1007/BF02762623
17. Gonzalez, M., Moure, C., Jurado, J.R., and Duran, P., *J. Mater. Sci*., 1993, vol. 28, p. 3451. https://doi.org/10.1007/BF0115
18. Rossell, H.J., *J. Solid State Chem*., 1976, vol. 19, no. 2, p. 103. https://doi.org/10.1016/0022-4596(76)90156-0
19. Rejith, R., Krishnan, R.R., John, A., Thomas, J.K., and Solomon, S., *Ionics*, 2019, vol. 25, p. 5091. https://doi.org/10.1007/s11581-019-03097-z
20. Kong, S.L., Karatchevtseva, I., Gregg, D.J., Blackford, M.G., Holmes, R., and Triani, G., *J. Eur. Ceram. Soc*., 2013, vol. 33, p. 3273. https://doi.org/10.1016/j.jeurceramsoc.2013.05.011
21. Kaliyaperumal, C., Sankarakumar, A., and Paramasivam, T., *J. Alloys Compd*., 2020, vol. 813, article ID 152221. https://doi.org/10.1016/j.jallcom.2019.152221
22. Heinicke, G., *Tribochemistry*, Berlin: Akademie, 1984.
23. *Fundamental'nye osnovy mekhanicheskoi aktivatsii, mekhanosinteza i mekhanokhimicheskikh tekhnologii* (Fundamentals of Mechanical Activation, Mechanosynthesis, and Mechanochemical Technologies), Avvakumov, E.G., Ed., Novosibirsk: Sib. Otd. Ross. Akad. Nauk, 2009.
24. Lapshin, O.V., Boldyreva, E.V., and Boldyrev, V.V., *Russ. J. Inorg. Chem*., 2021, vol. 66, p. 433. https://doi.org/10.1134/S0036023621030116
25. Salazar-Zertuche, M., Diaz-Guillen, J.A., Acosta-García, J.O., Diaz-Guillen, J.C., Montemayor, S.M., Burciaga-Diaz, O., Bazaldua-Medellin, M.E., and Fuentes, A.F., *Int. J. Hydrogen Energy*, 2019, vol. 44, no. 9, p. 12500. https://doi.org/10.1016/j.ijhydene.2018.11.141

26. Kaminskii, Yu.D., *Mekhanokhimicheskie reaktory planetarnogo tipa. Teoriya i praktika* (Planetary Mechanochemical Reactors. Theory and Practice), Novosibirsk: Nauka, 2015.
27. Kalinkin, A.M., Usoltsev, A.V., Kalinkina, E.V., Nevedomskii, V.N., and Zalkind, O.A., *Russ. J. Gen. Chem*., 2017, vol. 87, no. 10, p. 2258. https://doi.org/10.1134/S1070363217100024
28. Kalinkin, A.M., Vinogradov, V.Yu., and Kalinkina, E.V., *Inorg. Mater*., 2021, vol. 57, no. 2, p. 178. https://doi.org/10.1134/S0020168521020072
29. Dorofeev, G.A., Streletskii, A.N., Povstugar, I.V., Protasov, A.V., and Elsukov, E.P., *Colloid J*., 2012, vol. 74, no. 6, p. 678. https://doi.org/10.1134/S1061933X12060051
30. Avvakumov, E.G., *Mekhanicheskie metody aktivatsii khimicheskikh protsessov* (Mechanical Methods of Activation of Chemical Processes), Novosibirsk: Nauka, 1986.